J Fluoresc (2015) 25:1191–1201
DOI 10.1007/s10895-015-1606-1

ORIGINAL ARTICLE

Pyridine Based Fluorescence Probe: Simultaneous Detection and Removal of Arsenate from Real Samples with Living Cell Imaging Properties

Sandip Nandi[1] · Animesh Sahana[1] · Bidisha Sarkar[2] · Subhra Kanti Mukhopadhyay[2] · Debasis Das[1]

Published online: 24 July 2015

Abstract Pyridine based fluorescence probe, **DFPPIC** and its functionalized Merrifield polymer has been synthesized, characterized and used as an arsenate selective fluorescence sensor. Arsenate induced fluorescence enhancement is attributed to inter-molecular H-bonding assisted CHEF process. The detection limit for arsenate is 0.001 μM, much below the WHO recommended tolerance level in drinking water. **DFPPIC** can detect intracellular arsenate in drinking water of Purbasthali, West Bengal, India efficiently.

Keywords Fluorescence probe · Intracellular arsenate imaging · Merrifield resin · Visible light excitation

Introduction

Arsenic (As), a highly poisonous element in mineral and soil can easily percolate into water. In nature, it is widely distributed as organic and inorganic (As^{III} or As^{V}) species [1]. However, natural abundance of inorganic As species are higher. It is well known that arsenite (AsO_3^{3-}) and arsine (AsH_3) dominate at reducing atmosphere while arsenate (AsO_4^{3-}) in oxygenized environments [2, 3]. Consumption of low levels As over a longer period is harmful with a high risk of cancer [4]. World Health Organizations (WHO) prescribed 10 ppb as the highest tolerance level for As in drinking water [5]. Hence, determination of As at ppb level is of utmost importance and challenging.

The available methods for such trace level determination of As use sophisticated, expensive equipment that require longer analysis time restricting them for on-site field detection, particularly in developing countries.

On the other hand, fluorescence method being simple, less expensive, non-destructive, and user friendly, it requires short analysis time to achieve low detection limit. Moreover, it is also useful for in-vivo studies. Hence, this method is becoming very popular in environmental science, medicine and biology [6–9].

Design of fluorescence probe is commonly based on intramolecular charge transfer (ICT) [10, 11], photo induced electron transfer (PET) [12–15], chelation enhanced fluorescence (CHEF) [16–19], metal-ligand charge transfer (MLCT) [20, 21], excimer/ exciplex formation [22–25], intermolecular hydrogen bonding [26], excited-state intra-molecular proton transfer (ESIPT) [27], displacement approach [28], and fluorescence resonance energy transfer (FRET) [29–38] mechanism.

Presently we are actively engaged to develop low cost arsenate selective 'turn on' fluorescent probe [39–42] having lowest detection limit less than the WHO recommended tolerance level in drinking water. We have also undertaken the challenge to use the same probe for removal of arsenate from real drinking water samples and imaging of living cells contaminated with arsenate as well. Additionally, visible light excitable, water soluble probe appears to be harmless to the living cells studied.

✉ Debasis Das
ddas100in@yahoo.com

[1] Department of Chemistry, The University of Burdwan, Golapbag, Burdwan, India

[2] Department of Microbiology, The University of Burdwan, Golapbag, Burdwan, India

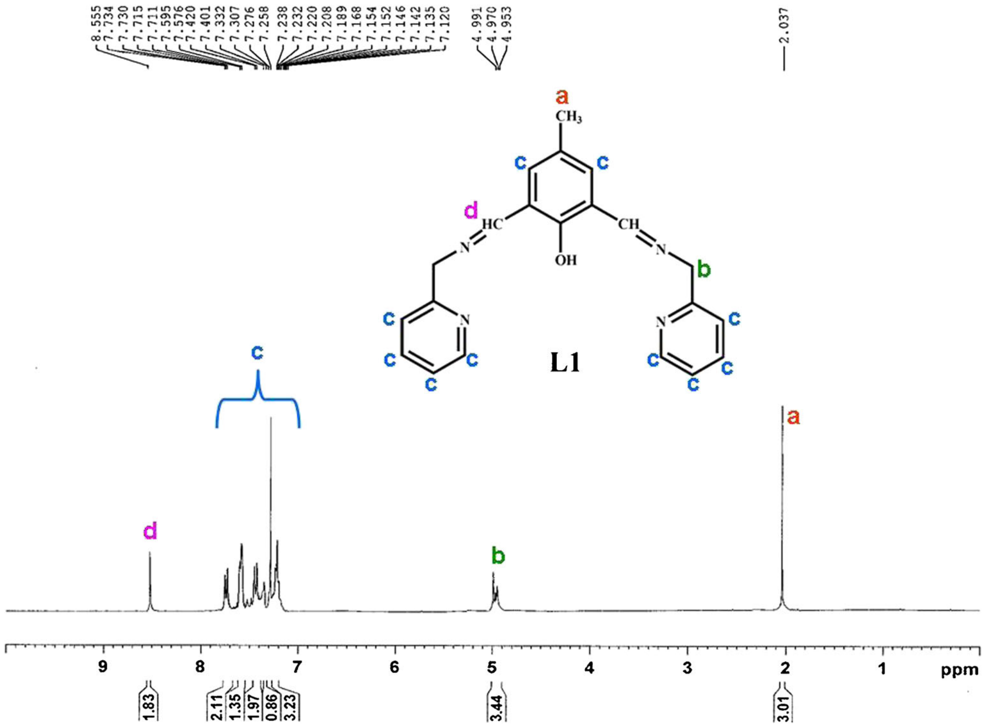

Fig. 1 [1]H NMR spectrum of **DFPPIC** in $CDCl_3$

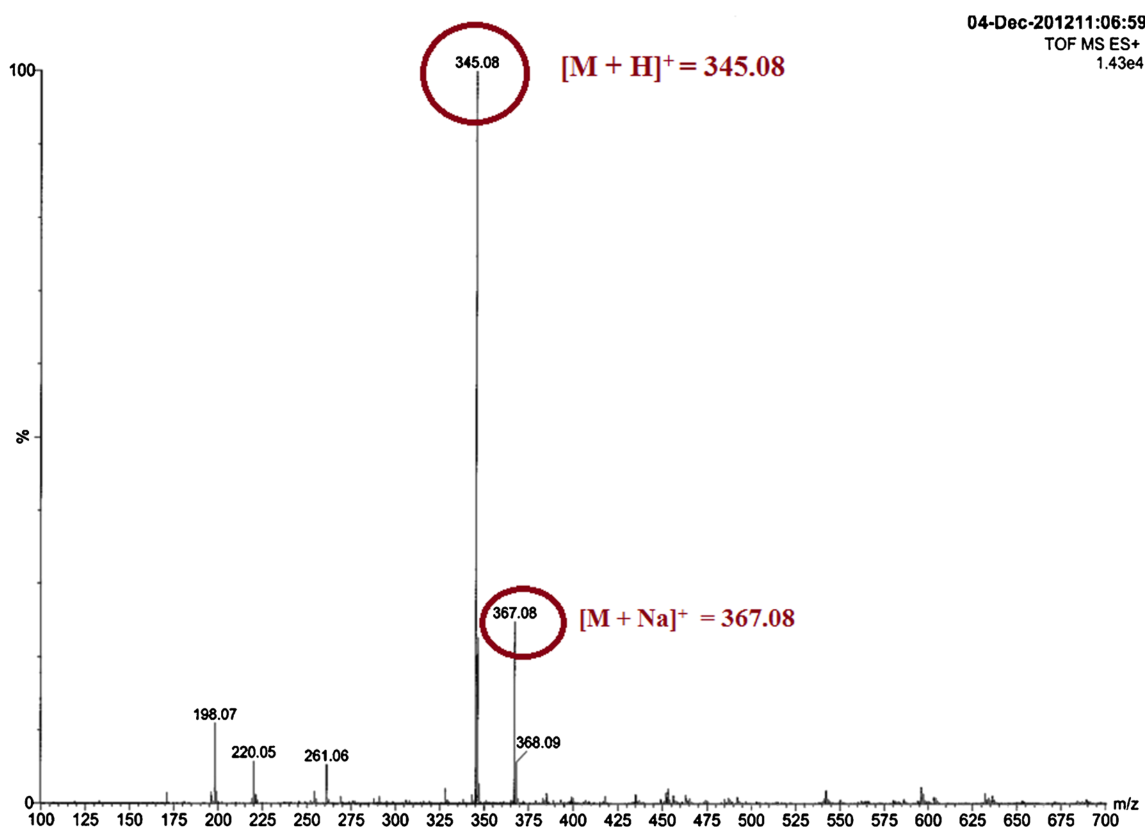

Fig. 2 QTOF-MS spectrum of **DFPPIC**

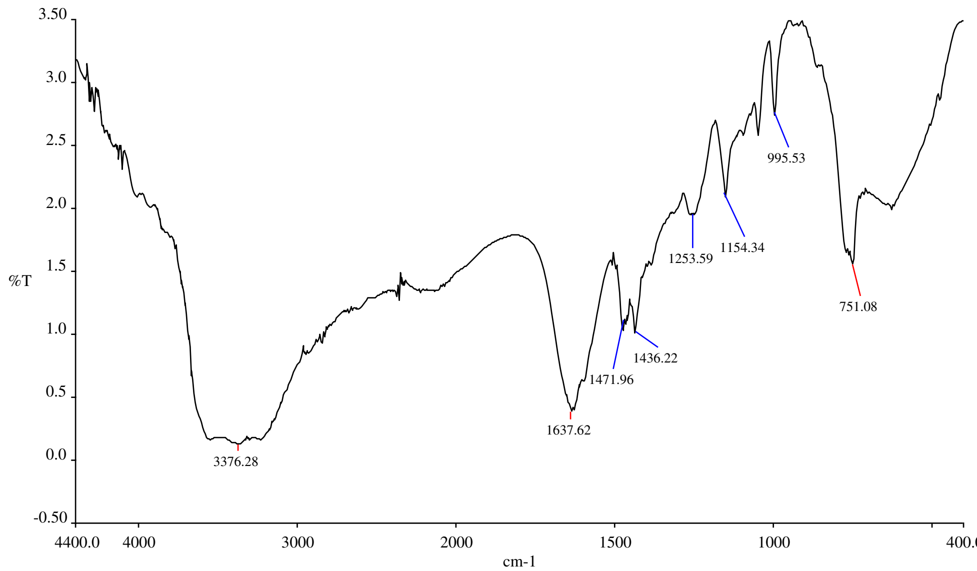

Fig. 3 FTIR spectrum of **DFPPIC**

Experimental

Reagents and Solution

High-purity HEPES, *p*-cresol and 2-picolyl amine are purchased from Sigma Aldrich (India). NaH_2AsO_4 is purchased from Merck (India). Solvents used are of spectroscopic grade. Other chemicals are analytical reagent grade and have been used without further purification except when specified. Mili-Q Milipore® 18.2 MΩ cm^{-1} water is used throughout the experiments.

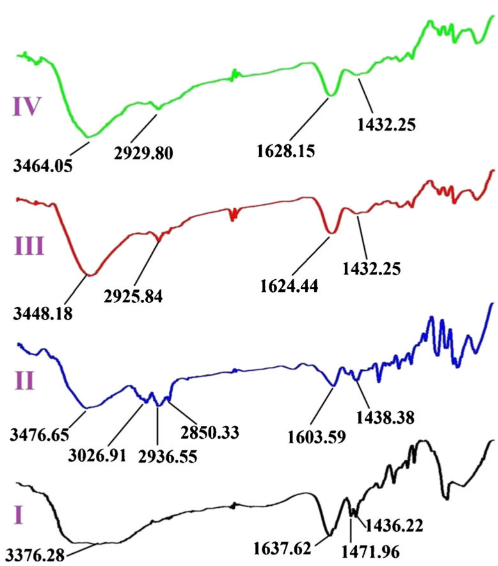

Fig. 4 FTIR spectra of (I) free **DFPPIC**, (II) free **Merifield polymer**, (III) **DFPPIC-Merifield polymer** and (III) **DFPPIC-Merifield polymer**+$H_2AsO_4^-$

Instrumentation and Apparatus

FTIR spectra are recorded on a SHIMADZU FTIR spectrometer (model: FTIR-H20). Mass spectra are performed on a QTOF Micro YA 263 mass spectrometer in ES positive mode. Scanning electron microscope (Hitachi S-530, Japan) is used to capture SEM images. Samples for SEM images are prepared using gold coating IV2 instrument. ^1H NMR spectra are recorded using Bruker Avance 400 (400 MHz) in $CDCl_3$ and MeOD. Melting point measurement is done by VEEGO digital melting point apparatus. Elemental analysis is performed using Perkin Elmer CHN-Analyzer with first 2000-Analysis kit. The steady-state fluorescence emission and excitation spectra are recorded with a Perkin Elmer Precisely LS55 spectrofluorimeter. A SHIMADZU (model -2450) UV–Vis spectrophotometer has been used for measuring the absorption spectra. All pH measurements are performed with Systronics digital pH meter (model 335).

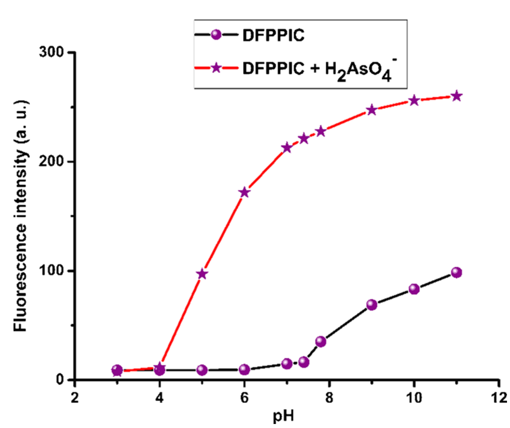

Fig. 5 Variation of emission intensity of **DFPPIC** (1 μM) in presence of $H_2AsO_4^-$ (500 μM) as a function of pH, λ_{ex}=400 nm

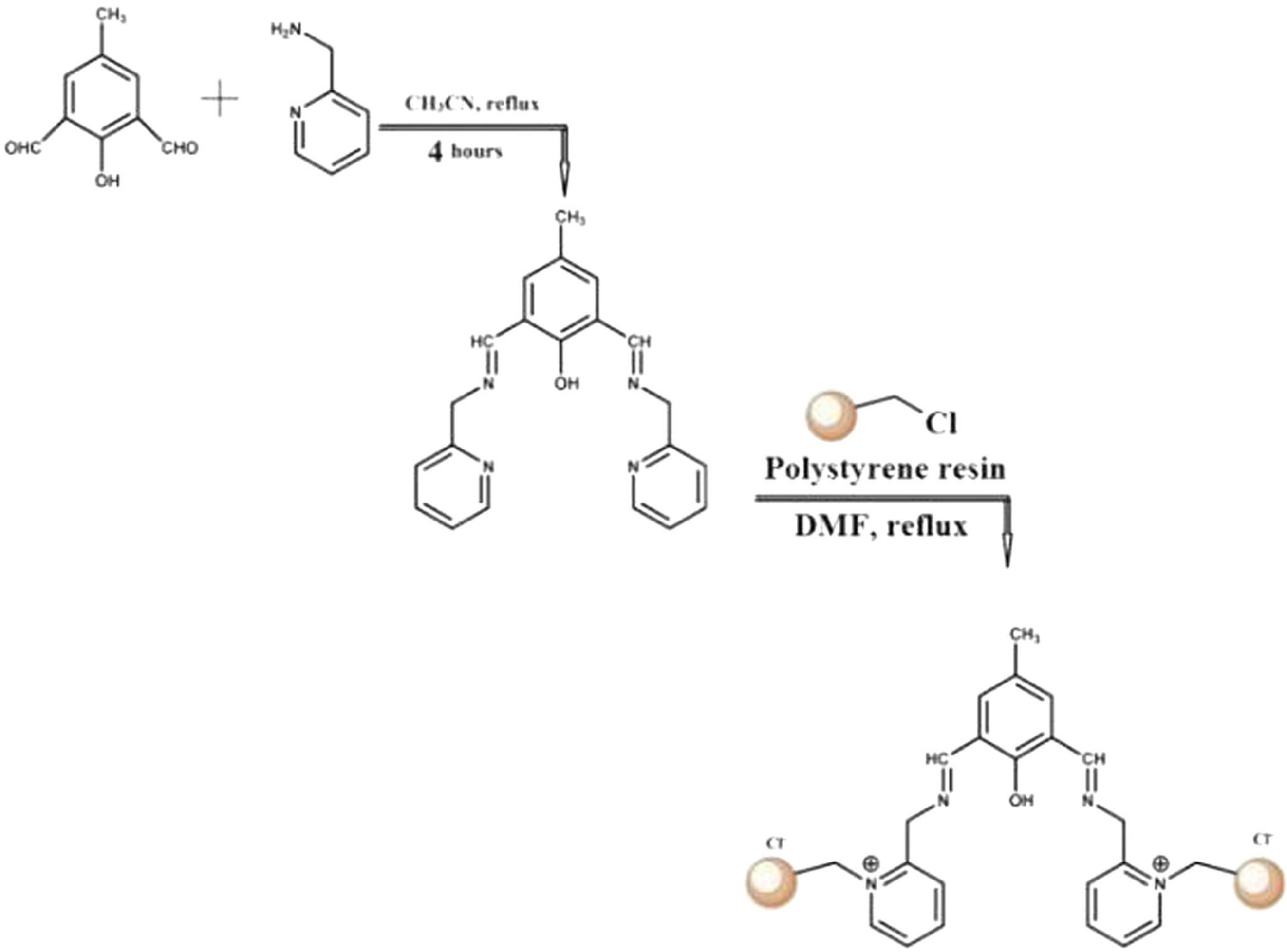

Scheme 1 Synthesis of **DFPPIC** and **DFPPIC** appended resin

Synthesis of 4-methyl-2, 6-bis((E) -(pyridin-2-ylmethylimino)methyl)phenol (DFPPIC)

2, 6-Diformyl-4-methylphenol was prepared by modification of the literature method [43].

To a solution of 2-picolyl amine (0.133 g, 1.23 mmol) in acetonitrile (10 mL), 10 mL acetonitrile solution of di-formyl *p*-cresol (0.100 g, 0.617 mmol) is added dropwise. The reaction mixture is refluxed for 4 h to form a yellow precipitate. The solid is filtered, washed with ethanol thrice. Crude product is purified by re-crystallization from acetonitrile to give 0.193 g of **DFPPIC** (yellow solid) in 82.8 % yield; M. P. 143 °C (±4 °C); ^{1}H NMR (400 MHz, $CDCl_3$) (Fig. 1), 2.03 (3H, s, a); 4.99 (4H, m, J=10.0 Hz, b); 7.73~7.12 (10H, m, J=10.0 Hz, c); 8.55 (2H, s, d); QTOF – MS ES$^+$ (Fig. 2): $[M+H]^+$=345.08; $[M+Na]^+$=367.08; elemental analysis data as calculated for $C_{21}H_{20}N_4O$ (%): C, 73.23; H, 5.85 and N, 16.27. Found (%): C, 73.11; H, 5.89 and N, 16.21. FTIR/ cm^{-1} (Fig. 3): υ(OH) 3376.28, υ(C=N) 1637.62.

Synthesis of DFPPIC Appended Merrifield Resin

DFPPIC (100 mg) is appended on Merrifield resin by refluxing a DMF solution of **DFPPIC** with chloromethyl polystyrene. Filtration of the reaction mixture followed by

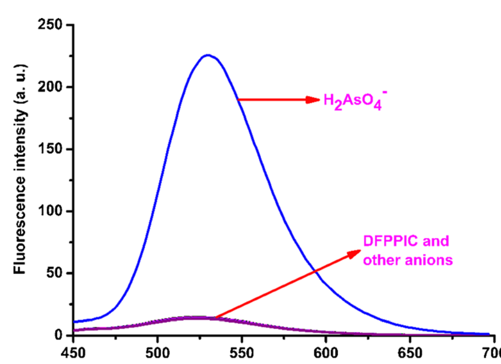

Fig. 6 Changes in the emission spectra of **DFPPIC** (1 μM) in presence of different anions (500 μM) in HEPES buffered solution (0.1 M, ethanol/water=1/9, *v*/*v*, pH 7.4), where other anions=F^-, Cl^-, Br^-, I^-, N_3^-, NO_2^-, NO_3^-, SCN^-, CN^-, CH_3COO^-, ClO_4^-, $H_2PO_4^-$, λ_{ex}=400 nm

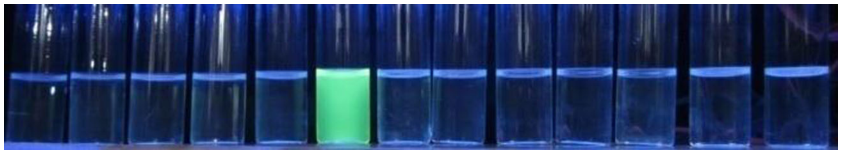

Fig. 7 Observed colors of **DFPPIC** (1 μM) under a hand held UV lamp in presence of different anions (500 μM): (from left to right), F^- **(1)**, Cl^- **(2)**, Br^- **(3)**, I^- **(4)**, N_3^- **(5)**, $H_2AsO_4^-$ **(6)**, CH_3COO^- **(7)**, NO_3^- **(8)**, SCN^- **(9)**, CN^- **(10)**, ClO_4^- **(11)**, $H_2PO_4^-$ **(12)** and NO_2^- **(13)**

thorough washing with DMF to remove unreacted **DFPPIC** has yielded the target polymer. Finally, the beads are washed properly with water and diethyl ether to have the desired Merrifield polymer bound host **DFPPIC**. The beads are characterized by FTIR and SEM. FTIR spectrum of **DFPPIC** (Fig. 4) show the peaks at 3076.28 and 1637.62 cm^{-1} which are attributed to –OH and –C=N functionalities. After sorption of arsenate, the significant shift of –OH peak (3476.28 $cm^{-1} \rightarrow$ 3464.05 cm^{-1}) and imine peaks (1637.62 $cm^{-1} \rightarrow$ 1628.15 cm^{-1}) have been observed which support the binding of arsenate by **DFPPIC-**resin. Changes in the morphology in the SEM images and emission of green light from the arsenate sorbed beads under fluorescence microscope further support the fact.

General Method of UV–Vis and Fluorescence Titration

Path length of the cells used for absorption and emission studies is 1 cm. For UV–Vis and fluorescence titrations, stock solution of **DFPPIC** is prepared (10 μM) in ethanol/water (1/9, *v*/*v*) HEPES (0.1 M) buffer. Working solutions of **DFPPIC** and $H_2AsO_4^-$ are prepared from their respective stock solutions. Fluorescence measurements are performed using 10 nm×10 nm slit width. All the fluorescence and absorbance spectra are recorded after 5 min of mixing of $H_2AsO_4^-$ to **DFPPIC**.

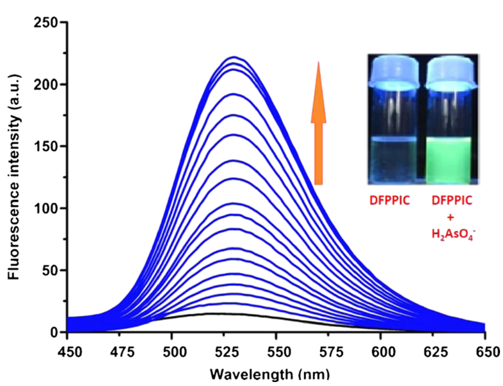

Fig. 8 Changes of the emission spectra of **DFPPIC** (1 μM) upon gradual addition of $H_2AsO_4^-$ (0, 0.001, 0.01, 0.1, 1, 5, 10, 15, 25, 30, 40, 50, 70, 90, 100, 150, 300, 500 μM) in HEPES buffered (0.1 M, ethanol/water=1/9, *v*/*v*, pH 7.4). Inset: color changes of **DFPPIC** in presence of $H_2AsO_4^-$ under a hand held UV lamp, λ_{ex}=400 nm

Calculation of Quantum Yield

Fluorescence quantum yields (Φ) are estimated by integrating the area under the fluorescence curves using the equation,

$$\phi\text{sample} = \phi\text{ref} \times \frac{\text{ODref} \times \text{Asample} \times \eta^2\text{sample}}{\text{ODsample} \times \text{Aref} \times \eta^2\text{ref}}$$

where A is the area under the fluorescence spectral curve, OD is optical density of the compound at the excitation wavelength [44] and η is the refractive indices of the solvent. Anthracene is used as quantum yield standard (quantum yield is 0.27 in ethanol) [45] for measuring the quantum yields of **DFPPIC** and [**DFPPIC** -$H_2AsO_4^-$] systems.

Job's Plot from Fluorescence Experiments

A series of solutions containing **DFPPIC** and $H_2AsO_4^-$ have been prepared such that the total concentration of $H_2AsO_4^-$ and **DFPPIC** remain constant (10 μM) in all the sets. The mole fraction (X) of **DFPPIC** is varied from 0.1 to 0.9. The emission intensity at 530 nm is plotted against the mole fraction of **DFPPIC** in solution.

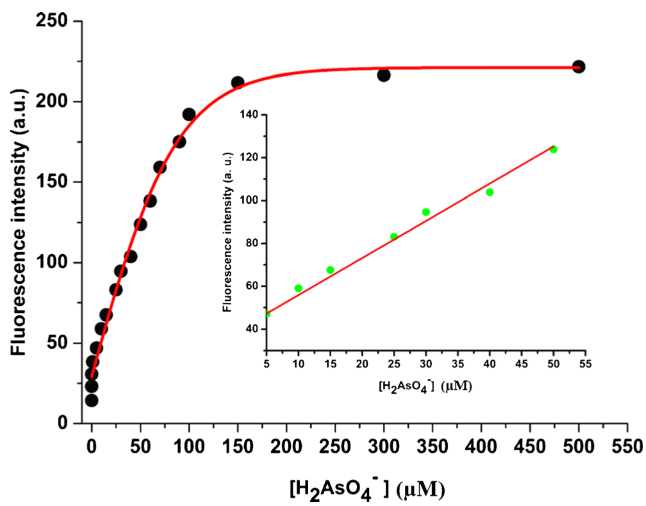

Fig. 9 Plot of emission intensities of **DFPPIC** (1 μM) with increasing concentration of $H_2AsO_4^-$ (0, 0.001, 0.01, 0.1, 1, 5, 10, 15, 25, 30, 40, 50, 70, 90, 100, 150, 300, 500 μM) in HEPES buffered (0.1 M, ethanol/water=1/9, *v*/*v*, pH 7.4) solution. Inset: linear region from 0.001 to 100 μM of $H_2AsO_4^-$, λ_{ex}=400 nm, λ_{em}=530 nm

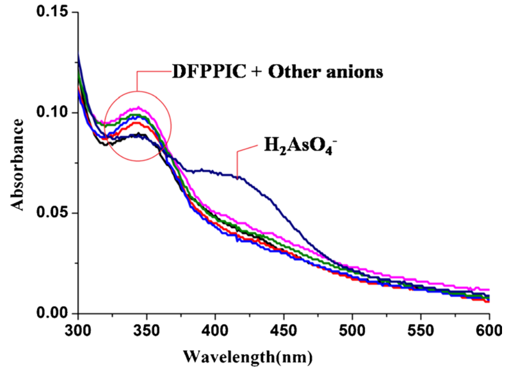

Fig. 10 Absorbance of the **DFPPIC** (10 μM) in presence of different anions (1000 μM) in HEPES buffered solution (0.1 M, ethanol/water=1/9, *v/v*, pH 7.4), other anions are F^-, Cl^-, Br^-, I^-, N_3^-, NO_2^-, NO_3^-, SCN^-, CN^-, CH_3COO^-, ClO_4^- and $H_2PO_4^-$

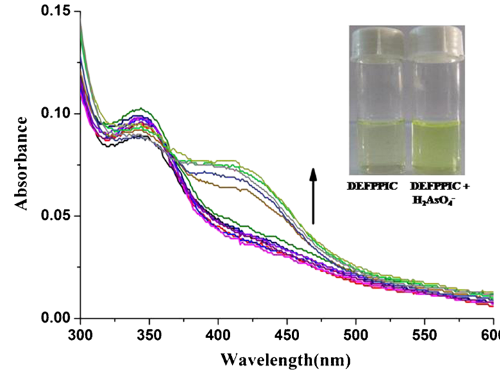

Fig. 12 Changes of the absorption spectra of **DFPPIC** (10 μM) upon gradual addition of $H_2AsO_4^-$ (0, 60, 70, 80, 90, 100, 200, 300 μM) in HEPES buffered (0.1 M, ethanol/water=1/9, *v/v*, pH 7.4). Inset: color changes of **DFPPIC** in presence of $H_2AsO_4^-$

Results and Discussion

Synthesis of the arsenate selective "off-on" probe, 4-methyl-2,6-bis((*E*)-(pyridin-2-ylmethylimino)methyl)phenol (**DFPPIC**) is shown in Scheme 1. Very weak emission (λ_{em}= 530 nm, λ_{ex}=400 nm) of **DFPPIC** with a quantum yield of 1.6×10^{-2} in HEPES buffered EtOH: water (0.1 M, 1:9, *v/v*, pH 7.4) solution is attributed to the PET process from N-center of pyridyl moiety to **DFP** unit.

As pH of the medium severely affects the efficiency of electron donor/ acceptor based fluorescence probes, pH of the sensing processes has been optimized. For this purpose, **DFPPIC** and $H_2AsO_4^-$ have been mixed in different sets at different pH (pH 3.0 -11.0). Figure 5 indicates a significant change of emission intensities that occur in the pH ranging 5.0 to 11.0. As living cell imaging studies are desirable in the vicinity of neutral pH, hence pH 7.4 is maintained throughout the entire studies.

Gradual addition of $H_2AsO_4^-$ to **DFPPIC** increases the emission intensities leading to 13.4 times enhancement of fluorescence quantum yield (21.3×10^{-2}), attributed to the intermolecular H-bonding assisted CHEF process leading to the inhibition of PET and enhanced rigidity of the molecular assembly causing restricted rotation around the azomethine functionality.

Selectivity of **DFPPIC** towards $H_2AsO_4^-$ over other common anions viz. F^-, Cl^-, Br^-, I^-, N_3^-, NO_2^-, NO_3^-, SCN^-, CN^-, CH_3COO^-,ClO_4^-, $H_2PO_4^-$ have been checked and presented in Fig. 6. Except $H_2AsO_4^-$, no other anions enhance the emission intensity of **DFPPIC**. Figure 7 clearly demonstrates that only $HAsO_4^{2-}$ is capable to emit green light upon interaction with **DFPPIC**, observed under UV lamp.

Fluorescence titration reveals that gradual addition of $H_2AsO_4^-$ to **DFPPIC** enhances its emission intensity (Fig. 8) to a maximum at 500 μM. Plot of emission intensity as a function of $H_2AsO_4^-$ concentration is sigmoidal, the linear region (up to 50 μM $H_2AsO_4^-$) of which is useful for determination of unknown $H_2AsO_4^-$ concentration (Fig. 9). The same plot also allowed to measure arsenate as low as 1×10^{-9} M, lower than that of WHO recommended tolerance level in drinking water. Figure 10 illustrates the changes in the UV–Vis spectra of **DFPPIC** in presence of different common anions viz. F^-, Cl^-, Br^-, I^-, N_3^-, NO_2^-, NO_3^-, SCN^-, CN^-, CH_3COO^-, ClO_4^-, $H_2PO_4^-$ and $H_2AsO_4^-$ while the colors of the respective adducts are shown in Fig. 11. The absorption spectrum of free **DFPPIC** shows a broad peak at 342 nm. Gradual addition of $H_2AsO_4^-$ to **DFPPIC** reduces the intensity of 342 nm peak with the appearance of a new peak at 412 nm (Fig. 12), the intensity of which gradually increases with the increasing concentration of $H_2AsO_4^-$. Plot of absorbance (at 412 nm) of **DFPPIC** as a function of $H_2AsO_4^-$ concentration is also sigmoidal, the linear portion of which is useful for unknown $H_2AsO_4^-$ determination (Fig. 13).

Figure 14 clearly indicates that common tested anions do not interfere in the determination of $H_2AsO_4^-$. Interestingly, another similar anion, $H_2PO_4^-$ does not show any significant

Fig. 11 Observed colors of **DFPPIC** (10 μM) in presence of different anions (1000 μM): (from left to right), F^- **(1)**, Cl^- **(2)**, Br^- **(3)**, I^- **(4)**, N_3^- **(5)**,NO_3^- **(6)**, CH_3COO^- **(7)**, $H_2AsO_4^-$ **(8)**, SCN^- **(9)**, CN^- **(10)**, ClO_4^- **(11)**, $H_2PO_4^-$ **(12)**, NO_2^- **(13)**, **DFPPIC (14)**

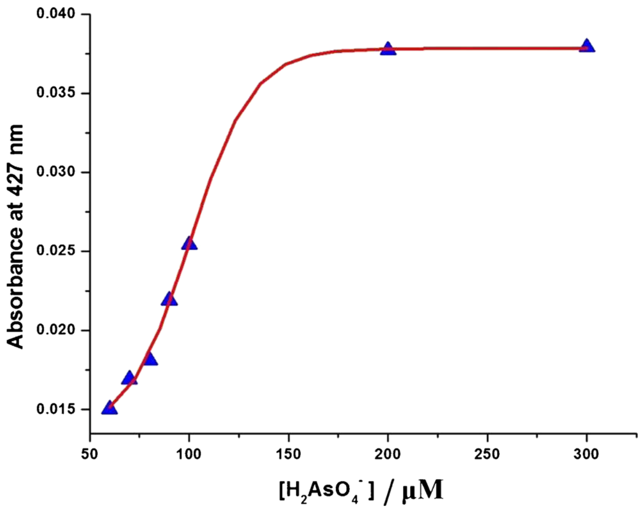

Fig. 13 Plot of absorbance of **DFPPIC** (10 μM) with increasing concentration of $H_2AsO_4^-$ (0, 60, 70, 80, 90, 100, 200, 300 μM) in HEPES buffered (0.1 M, ethanol/water=1/9, *v/v*, pH 7.4, λ=427 nm)

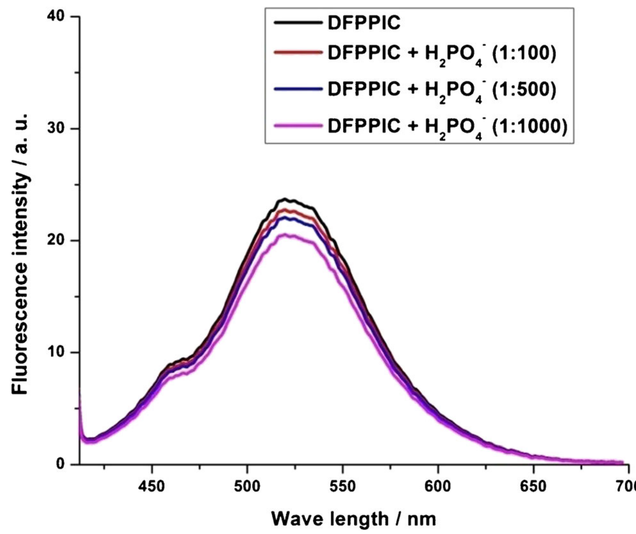

Fig. 15 Changes of the emission spectra of **DFPPIC** (10 μM) upon gradual addition of $H_2PO_4^-$ (0, 100, 500, 1000 μM) in HEPES buffered (0.1 M, ethanol/water=1/9, *v/v*, pH 7.4)

change of the emission intensity of **DFPPIC** (Fig. 15). Kim research group have already established that larger van der Waals radius of As increases the As-O distance, which is probably responsible for the differential interaction of phosphate and arsenate species [46]. In present case, plausibly this size factor allows arsenate but not phosphate to fit into the cavity of **DFPPIC** followed by its stabilization via intermolecular H-bonding (Fig. 16).

Job's plot indicates a 1:1 stoichiometry of the adduct formed between **DFPPIC** and $H_2AsO_4^-$ (Fig. 17). Binding constant of **DFPPIC** for $H_2AsO_4^-$ is estimated using modified Benesi-Hildebrand [47] equation: $(F_{max}- F_0)/ (F_x-F_0)=1+(1/K) (1/[M]^n)$ where $F_{max,}$ F_0, F_x are emission intensity of **DFPPIC** in presence of $H_2AsO_4^-$ at saturation, free **DFPPIC** and at any intermediate $H_2AsO_4^-$ concentration. Plot of $(F_{max} - F_0)/ (F_x-F_0)$ vs. $1/ [M]^{1/2}$ (here, n=1/2) have yielded the binding constant as 1.32×10^4 M^{-1} (R^2=0.9894) (Fig. 18), indicating a significant interaction between **DFPPIC** and $H_2AsO_4^-$. Mass spectrum of the [**DFPPIC** -$H_2AsO_4^-$] adduct have supported our conclusion (Fig. 19).

Figure 20 clearly demonstrates that **DFPPIC** is very useful to detect intracellular $H_2AsO_4^-$ in living cells, grown in arsenate contaminated water collected from Purbasthali, a highly arsenic contaminated area in west Bengal, India [48]. Thus, **DFPPIC** can easily permeate through the cell membrane to stain intracellular arsenate. The developed method may be very useful to determine trace level arsenate in drinking water.

Comparison of the SEM images (Fig. 21), fluorescence microscope images (Fig. 22) and FTIR spectra (Fig. 4) of free **DFPPIC**-Merrifield polymer with its arsenate loaded forms clearly indicates the sorption of arsenate on the **DFPPIC**-Merrifield polymer. Completely different morphology and intense green fluorescence of arsenate loaded **DFPPIC**-Merrifield polymer beads indicate the sorption of arsenate by the polymer.

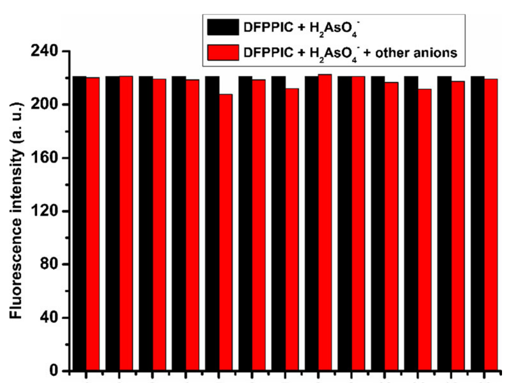

Fig. 14 Anion selectivity of **DFPPIC** (1 μM) in HEPES buffer (0.1 M; EtOH–H_2O, 1: 9*v/v*; pH 7.4. Black bars represent emission intensity of [**DFPPIC**-$H_2AsO_4^-$] system and red bars show the emission intensity of [**DFPPIC**-$H_2AsO_4^-$] system in presence of 500 μM of different anion: F^- **(1)**, Cl^- **(2)**, Br^- **(3)**, I^- **(4)**, N_3^- **(5)**, NO_2^- **(6)**, NO_3^- **(7)**, SCN^- **(8)**, CN^- **(9)**, CH_3COO^-**(10)**, SO_4^{2-} **(11)**, ClO_4^- **(12)**, and HPO_4^{2-} **(13)** (λ_{ex}= 400 nm, λ_{em}=530 nm)

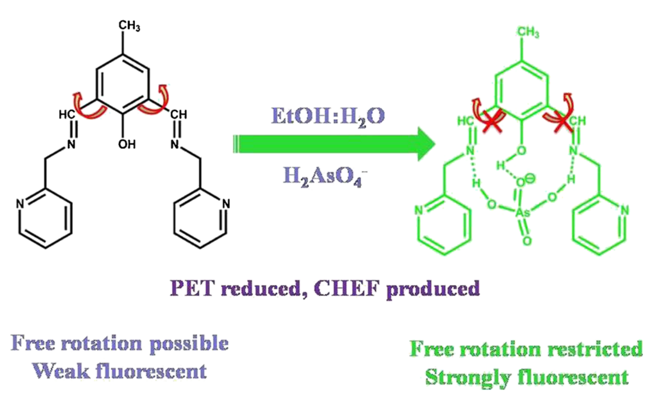

Fig. 16 Probable mechanism of binding interaction between **DFPPIC** and $H_2AsO_4^-$

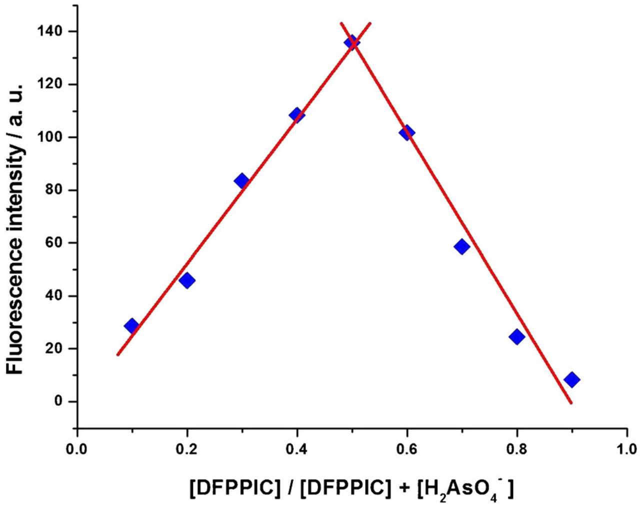

Fig. 17 Job's plot (stoichiometry determination of the [**DFPPIC**-$H_2AsO_4^-$] adduct) in HEPES buffer (0.1 M, ethanol/water=1/9, *v/v*, pH 7.4)

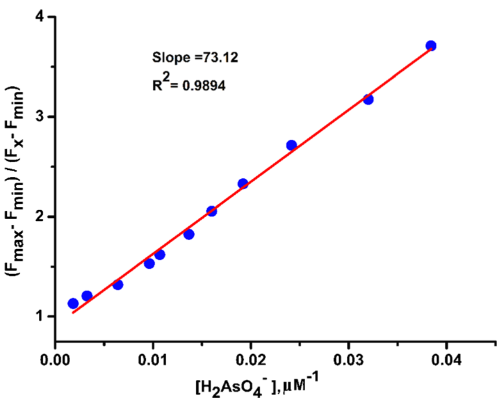

Fig. 18 Determination of binding constant between **DFPPIC** and $H_2AsO_4^-$ in HEPES buffered (0.1 M, ethanol/water=1/9, *v/v*, pH 7.4, λ_{ex}=400 nm, λ_{em}=530 nm)

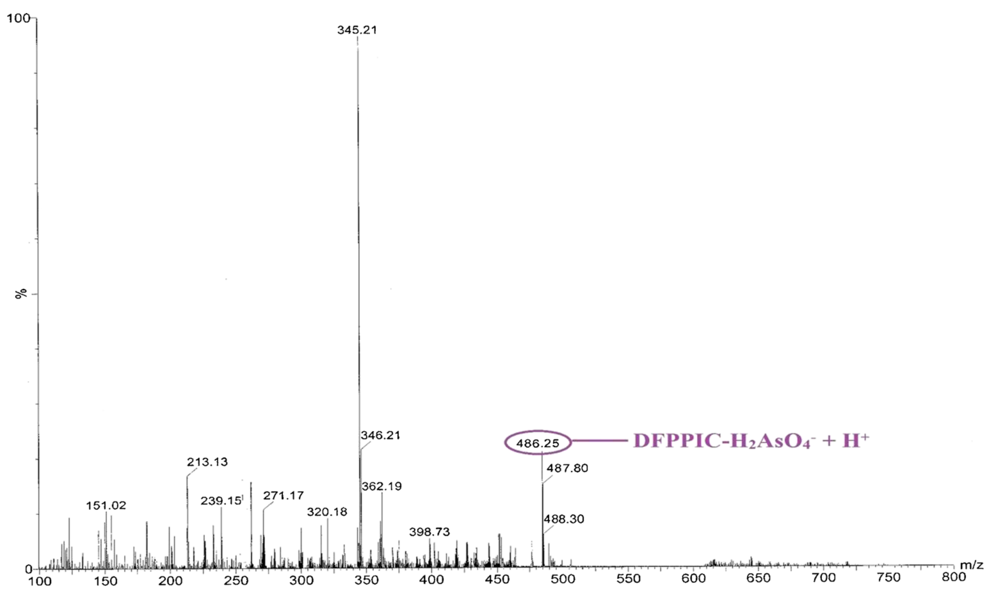

Fig. 19 QTOF-MS spectrum of [**DFPPIC**-$H_2AsO_4^-$] adduct

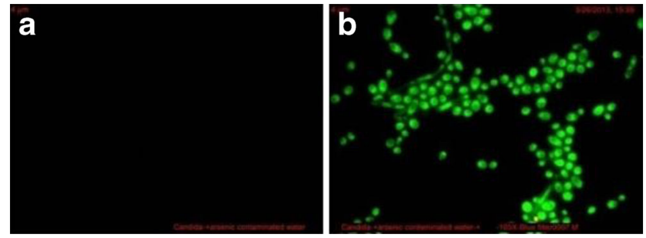

Fig. 20 Fluorescence microscope images of *Candida albicans* (IMTECH No. 3018) cells grown in arsenic contaminated water collected from Purbasthali, **a** without treatment of **DFPPIC** and **b** after treatment with **DFPPIC**. Incubation temperature, 37 °C

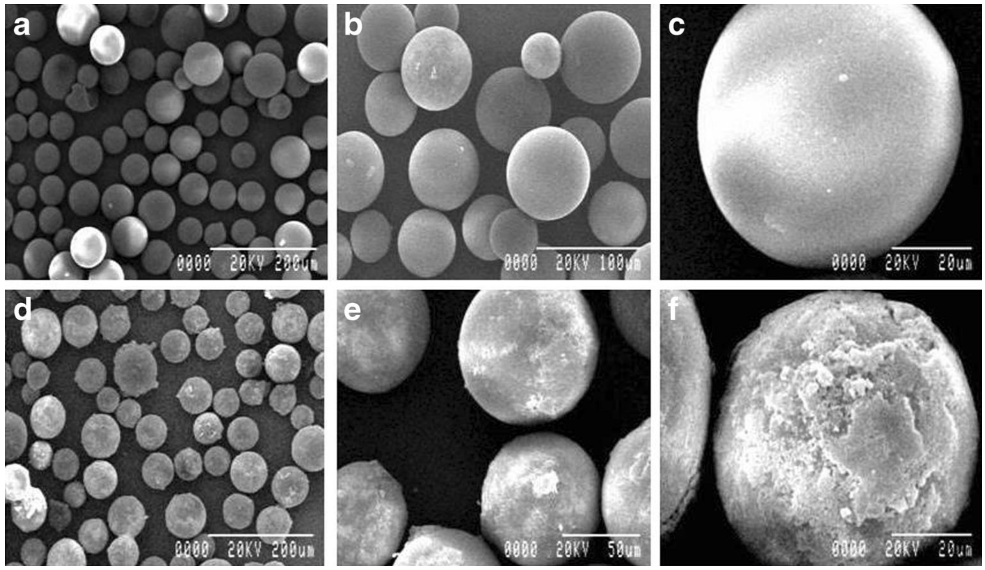

Fig. 21 (**a**), (**b**) and (**c**) are the SEM images of the free **DFPPIC** resin. (**d**), (**e**) and (**f**) are the SEM images of the arsenate loaded **DFPPIC** resin. Significant changes in the morphology of resin beads indicate the sorption of $H_2AsO_4^-$ on **DFPPIC** resin

Application

Cell Imaging Studies

Imaging System

The imaging system is composed of an inverted fluorescence microscope (Leica DM 1000 LED), digital compact camera (Leica DFC 420C), and an image processor (Leica Application Suite v3.3.0). The microscope is equipped with a 50 W mercury arc lamp.

Preparation of Samples from Arsenic Contaminated Water Collected Form Purbasthali, India

Candida albicans cells (IMTECH No. 3018) from exponentially growing culture in yeast extract glucose broth medium (pH 6.0, incubation temperature, 37 °C) are centrifuged at 3000 rpm for 10 min and washed twice with 0.1 M HEPES buffer (pH 7.4). Cells are treated with 1 % saline water for cleaning. Then, cells are incubated in 500 μL arsenic contaminated water for overnight. Cells thus obtained are mounted on grease free glass slide and observed under the fluorescence microscope having UV filter. Cells incubated without **DFPPIC** are used as control.

Removal of Arsenate from Drinking Water of Purbasthali Using DFPPIC-Merrifield Polymer

50 mg of **DFPPIC** appended Merrifield polymer is taken in a 50 mL beaker. 5.0 mL clean arsenic contaminated drinking water is added to the beaker containing **DFPPIC**-Merrifield polymer and kept for 6 h under stirring conditions. After filtration, arsenate sorbed **DFPPIC**-Merrifield polymer is dried. The concentration of arsenate in the drinking water is measured before and after sorption using the developed Moreover, arsenate sorbed polymer beads are subjected to SEM and observed under fluorescence microscope. Both the images indicated that arsenate is sorbed on the polymer. The arsenate sorbed polymer beads emit green color under fluorescence microscope. The morphology and surface of the arsenate sorbed beads changes significantly.

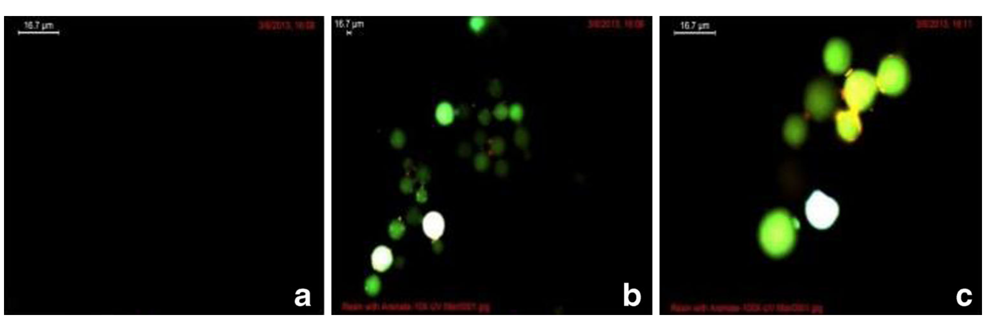

Fig. 22 **a** Fluorescence microscope images of **DFPPI**C-Merrifield polymer before sorption of $H_2AsO_4^-$; **b** fluorescence microscope images of **DFPPI**C-Merrifield polymer after sorption of $H_2AsO_4^-$ at 10× objective lens and **c** the system **b** observed under 100× objective lens

Conclusion

DFPPIC and its Merrifield polymer has been synthesized and used as an arsenate selective fluorescence sensor. Arsenate induced fluorescence enhancement is attributed to intermolecular H-bonding assisted CHEF process. The detection limit for arsenate is 0.001 μM, much below the WHO recommended tolerance level in drinking water. **DFPPIC** can detect very efficiently intracellular arsenate in organelles grown in water collected from Purbasthali, a highly arsenic contaminated region of India. Removal of arsenate from real samples have also been achieved using **DFPPIC** appended Merrifield polymer. Simultaneous determination and removal of trace level arsenate in contaminated real samples has been established by SEM, fluorescence microscope and FTIR spectral studies.

Acknowledgments Financial support from DST (Govt. of West Bengal) is gratefully acknowledged. S. Nandi and A. Sahana are grateful to UGC and CSIR, New Delhi for fellowship. We thank CAS (B. U.) for infrastructural and financial help.

References

1. Ensafi AA, Ring AC, Fritsch I (2010) Highly sensitive voltammetric speciation and determination of inorganic arsenic in water and alloy samples using ammonium 2-amino-1-cyclopentene-1-dithiocarboxylate. Electroanal 22(1175):1185
2. Boyle RW, Jonasson IR (1973) The geochemistry of arsenic and its use as an indicator element in geochemical prospecting. J Geochem Explor 2(251):296
3. Hasegawa H, Matsui M, Okamura S, Hojo M, Iwasaki N, Sohrin Y (1999) Arsenic speciation including 'hidden' arsenic in natural water. Appl Organomet Chem 13(113):119
4. Morales KH, Ryan L, Kuo TL, Wu MM, Chen CJ (2000) Risk of internal cancers from arsenic in drinking water. Environ Health Perspect 108(655):661
5. WHO (2011) Guidelines for drinking-water quality, 4th ed.; World Health Organization: Geneva, Switzerland
6. Quang DT, Kim JS (2010) Fluoro- and chromogenic chemodosimeters for heavy metal ion detection in solution and bio-specimens. Chem Rev 110(6280):6301
7. Kobayashi H, Ogawa M, Alford R, Choyke PL, Urano Y (2010) New strategies for fluorescent probe design in medical diagnostic imaging. Chem Rev 110(2620):6240
8. Callan JF, Silva APD, Magri DC (2005) Luminescent sensors and switches in the early 21st century. Tetrahedron 61(8551):8588
9. Demchenko AP (2008) Introduction to fluorescence sensing. Springer, New York
10. Xu Z, Xiao Y, Qian X, Cui J, Cui D (2005) Ratiometric and selective fluorescent sensor for Cu^{II} based on internal charge transfer (ICT). Org Lett 7(889):892
11. Wang JB, Qian XF, Cui JN (2006) Detecting Hg^{2+} ions with an ICT fluorescent sensor molecule: remarkable emission spectra shift and unique selectivity. J Org Chem 71(4308):4311
12. Gunnlaugsson T, Davis AP, Brien JEO, Glynn M (2002) Fluorescent sensing of pyrophosphate and bis-carboxylates with charge neutral PET chemosensors. Org Lett 4(2449):2452
13. Vance DH, Czarnik AW (1994) Real-time assay of inorganic pyrophosphatase using a high-affinity chelation-enhanced fluorescence chemosensor. J Am Chem Soc 116(9397):9398
14. Kim SK, Yoon J (2002) A new fluorescent PET chemosensor for fluoride ions. Chem Commun 770
15. Banerjee A, Sahana A, Das S, Lohar S, Guha S, Sarkar B, Mukhopadhyay SK, Mukherjee AK, Das D (2012) A naphthalene exciplex based Al^{3+} selective on-type fuorescent probe for living cells at the physiological pH range: experimental and computational studies. Analyst 137(2166):2175
16. Lim NC, Schuster JV, Porto MC, Tanudra MA, Yao L, Freake HC, Bruckner C (2005) Coumarin-based chemosensors for Zinc(II):toward the determination of the design algorithm for CHEF-type and ratiometric probes. Inorg Chem 44(2018):2030
17. Das S, Sahana A, Banerjee A, Lohar S, Guha S, Matalobos JS, Das D (2012) Thiophene anchored naphthalene derivative: Cr^{3+} selective turn-on fluorescent probe for living cell imaging. Anal Methods 4(2254):2258
18. Sahana A, Banerjee A, Das S, Lohar S, Karak D, Sarkar B, Mukhopadhyay SK, Mukherjee AK, Das D (2011) A naphthalene-based Al^{3+} selective fluorescent sensor for living cell imaging. Org Biomol Chem 9(5523):5529
19. Das S, Dutta M, Das D (2013) Fluorescent probes for selective determination of trace level Al^{3+}: recent developments and future prospects. Anal Methods 5(6262):6285
20. Beer PD (1998) Transition-metal receptor systems for the selective recognition and sensing of anionic guest species. Acc Chem Res 31(71):80
21. Kim MJ, Konduri R, Ye H, MacDonnell FM, Puntoriero F, Serroni S, Campagna S, Holder T, Kinsel G, Rajeshwar K (2002) Dinuclear ruthenium(II) polypyridyl complexes containing large, redox-active, aromatic bridging ligands: synthesis, characterization, and intramolecular quenching of MLCT excited states. Inorg Chem 41(2471):2476
22. Nishizawa S, Kato Y, Teramae N (1999) Fluorescence sensing of anions via intramolecular excimer formation in a pyrophosphate-induced self-assembly of a pyrene-functionalized guanidinium receptor. J Am Chem Soc 121(9463):9464
23. Wu JS, Zhou JH, Wang PF, Zhang XH, Wu SK (2005) New fluorescent chemosensor based on exciplex signaling mechanism. Org Lett 7(2133):2136
24. Schazmann B, Alhashimy N, Diamond D (2006) Chloride selective Calix[4]arene optical sensor combining urea functionality with pyrene excimer transduction. J Am Chem Soc 128(8607):8614
25. Banerjee A, Sahana A, Guha S, Lohar S, Hauli I, Mukhopadhyay SK, Matalobos JS, Das D (2012) Nickel(II)-induced excimer formation of a naphthalene-based fluorescent probe for living cell imaging. Inorg Chem 51(5699):5704
26. Sahana A, Banerjee A, Lohar S, Guha S, Das S, Mukhopadhyay SK, Das D (2012) Cd(II)-triggered excimer–monomer conversion of a pyrene derivative: time dependent red-shift of monomer emission with cell staining application. Analyst 137(3910):3913
27. Sahana A, Banerjee A, Guha S, Lohar S, Chattopadhyay A, Mukhopadhyay SK, Das D (2012) Highly selective organic fluorescent probe for azide ion: formation of a "molecular ring". Analyst 137(1544):1546
28. Peng X, Wu Y, Fan J, Tian M, Han K (2005) Colorimetric and ratiometric fluorescence sensing of fluoride: tuning selectivity in proton transfer. Org Chem 70(10524):10531
29. Das S, Guha S, Banerjee A, Lohar S, Sahana A, Das D (2011) 2-(2-Pyridyl) benzimidazole based Co(II) complex as an efficient fluorescent probe for trace level determination of aspartic and glutamic acid in aqueous solution: a displacement approach. Org Biomol Chem 9(7097):7104

30. Serin JM, Brousmiche DW, Frechet JMJ (2002) A FRET-based ultraviolet to near-infrared frequency converter. J Am Chem Soc 124(11848):11849
31. Albers AE, Okreglak VS, Chang CJ (2006) A FRET-Based approach to ratiometric fluorescence detection of hydrogen peroxide. J Am Chem Soc 128(9640):9641
32. Lee SH, Kim SK, Bok JH, Lee SH, Yoon J, Lee K, Kim JS (2005) Singlet oxygen generation via two-photon excited FRET. Tetrahedron Lett 46(8163):8167
33. Dichtel WR, Serin JM, Edder C, Frechet JMJ, Matuszewski M, Tan LS, Ohulchanskyy TY, Prasad PN (2004) Singlet oxygen generation via two-photon excited FRET. J Am Chem Soc 2004(126): 5380–5381
34. Suresh M, Mishra S, Mishra SK, Suresh E, Mandal AK, Shrivastav A, Das A (2009) Resonance energy transfer approach and a New ratiometric probe for Hg^{2+} in aqueous media and living organism. Org Lett 11(2740):2743
35. Mahato P, Saha S, Suresh E, Liddo RD, Parnigotto PP, Conconi MT, Kesharwani MK, Ganguly B, Das A (2012) Ratiometric Detection of Cr^{3+} and Hg^{2+} by a naphthalimide-rhodamine based fluorescent probe. Inorg Chem 51(1769):1777
36. Sreenath K, Allen J, Davidson RMW, Zhu L (2011) A FRET-based indicator for imaging mitochondrial zinc ions. Chem Commun 47: 11730–11732
37. Wandell RJ, Younes AH, Zhu L (2010) Metal - coordination - mediated sequential Chelation-enhanced fluorescence (CHEF) and fluorescence resonance energy transfer (FRET) in a heteroditopic ligand system. New J Chem 34(2176):2182
38. Lohar S, Banerjee A, Sahana A, Banik A, Mukhopadhyay SK, Das D (2013) A rhodamine–naphthalene conjugate as a FRET based sensor for Cr^{3+} and Fe^{3+} with cell staining application. Anal Methods 5(442):445
39. Sahana A, Banerjee A, Lohar S, Sarkar B, Mukhopadhyay SK, Das D (2013) Rhodamine-based fluorescent probe for Al^{3+} through time-dependent PET–CHEF–FRET processes and its cell staining application. Inorg Chem 52(3627):3633
40. Lohar S, Sahana A, Banerjee A, Banik A, Mukhopadhyay SK, Matalobos JS, Das D (2013) Antipyrine based arsenate selective fluorescent probe for living cell imaging. Anal Chem 85(1778): 1783
41. Sahana A, Banerjee A, Lohar S, Panja S, Mukhopadhyay SK, Matalobos JS, Das D (2013) Fluorescence sensing of arsenate at nanomolar level in a greener way, naphthalene based probe for living cell imaging. Chem Commun 49(7231):7233
42. Banerjee A, Sahana A, Lohar S, Panja S, Mukhopadhyay SK, Das D (2014) Visible light excitable fluorescence probe and its functionalized Merrifield polymer: selective sensing and removal of arsenate from real samples. RSC Adv 4(3887):3892
43. Denton DA, Suschitzky H (1963) Synthetic uses of polyphosphoric acid. J Chem Soc 4741:4743
44. Austin E, Gouterman M (1978) Porphyrins. XXXVII. Absorption and emission of weak complexes with acids, bases, and salts. Bioinorg Chem 9(281):298
45. Van Houten J, Watts RJ (1976) Temperature dependence of the photophysical and photochemical properties of the tris (2, 2′-bipyridyl) ruthenium(II) ion in aqueous solution. J Am Chem Soc 98(4853):4858
46. Park SW, Kim CW, Lee JH, Shim G, Kim KS (2011) Comparison of arsenic acid with phosphoric acid in the interaction with a water molecule and an alkali/alkaline-earth metal cation. J Phys Chem A 115(11355):11361
47. Benesi HA, Hildebrand JH (1949) A spectrophotometric investigation of the interaction of iodine with aromatic hydrocarbons. J Am Chem Soc 71(2703):2707
48. Biswas B (2010) West Bengal, India, Geomorphic controls of arsenic in ground water in Purbasthali I & II Blocks of Burdwan district. Int J Environ Sci 4(429):439